IOPscience iopscience.iop.org

Home Search Collections Journals About Contact us My IOPscience

Pacing control of sawtooth and ELM oscillations in tokamaks

This content has been downloaded from IOPscience. Please scroll down to see the full text.

2016 Plasma Phys. Control. Fusion 58 124004

(http://iopscience.iop.org/0741-3335/58/12/124004)

View the table of contents for this issue, or go to the journal homepage for more

Download details:

IP Address: 131.155.102.29
This content was downloaded on 03/05/2017 at 17:04

Please note that terms and conditions apply.

You may also be interested in:

Injection locking of the sawtooth period by means of modulated EC current drive
G. Witvoet, M. Lauret, M.R. de Baar et al.

Robust sawtooth period control based on adaptive online optimization
J.J. Bolder, G. Witvoet, M.R. de Baar et al.

Real-time control of ELM and sawtooth frequencies: similarities and differences
M. Lennholm, D. Frigione, J.P. Graves et al.

Systematic design of a sawtooth period feedback controller
G. Witvoet, M.R. de Baar, E. Westerhof et al.

Demonstration of sawtooth period locking with power modulation in TCV plasmas
M. Lauret, F. Felici, G. Witvoet et al.

Sawtooth period control strategies and designs for improved performance
G. Witvoet, M. Steinbuch, M.R. de Baar et al.

Chapter 3: MHD stability, operational limits and disruptions
T.C. Hender, J.C Wesley, J. Bialek et al.

Improved criterion for sawtooth trigger and modelling
A Zocco, J W Connor, C G Gimblett et al.

Chapter 8: Plasma operation and control
Y. Gribov, D. Humphreys, K. Kajiwara et al.

IOP Publishing Plasma Physics and Controlled Fusion
Plasma Phys. Control. Fusion **58** (2016) 124004 (9pp) doi:10.1088/0741-3335/58/12/124004

Pacing control of sawtooth and ELM oscillations in tokamaks

M Lauret[1], M Lennholm[2,3], M R de Baar[4,5] and W P M H Heemels[4]

[1] Department of Mechanical Engineering and Mechanics, Lehigh University, USA
[2] European Commission, B-1049 Brussels, Belgium
[3] EFDA Close Support Unit, Culham Science Centre, Abingdon, OX14 3DB, UK
[4] Department of Mechanical Engineering, Eindhoven University of Technology, PO Box 513, NL 5600 MB Eindhoven, The Netherlands
[5] FOM Institute DIFFER-Dutch Institute for Fundamental Energy Research, Association EURATOM-FOM, PO Box 1207, 3430 BE Nieuwegein, The Netherlands

E-mail: mennolauret@gmail.com

Received 21 February 2016, revised 22 April 2016
Accepted for publication 4 May 2016
Published 8 September 2016

Abstract

In tokamak plasmas, the sawtooth oscillation (ST) and the edge-localized-mode (ELM) are characterized by a phase of a slow evolution of the plasma conditions, followed by a crash-like instability that resets the plasma conditions when certain criteria of the plasma conditions are satisfied. Typically, the crashes induce losses of heat and energetic particles and may also trigger secondary instabilities. As the amplitude of the crash-like perturbation scales with the period between two crashes, period control of these oscillations is important for operations of large fusion facilities such as ITER and DEMO. In several present-day experimental facilities, a pacing control algorithm has been successfully applied for controlling the sawtooth period and the ELM period. However, a formal analysis has been lacking so far, which therefore forms the objective of the present paper. For this purpose, a reset model for the sawtooth period is introduced and, after a proper transformation a nonlinear discrete-time system is obtained, which is used for the formal analysis of pacing control. By representing the model in a Lur'e (or Lurie) form, we can derive conditions under which global asymptotic stability of the closed-loop (pacing) period control system is guaranteed. Moreover, we will show that the controller exhibits inherent robustness for model uncertainties. We envision that the analytical results in the area of pacing control of the sawtooth are also applicable to pacing period control of the ELM oscillation period. The presented reset model also explains why in recent experiments the sawtooth period locks with a periodically modulated power.

Keywords: sawtooth period control, pacing and period locking, ELM pacing, feedback control

(Some figures may appear in colour only in the online journal)

1. Introduction

For successful ITER operation, feedback control of several processes within the plasma and the magnetic field need to be effectively implemented. The evolution of the magnetic field and its coupling to the plasma on the macro-scale is well described by the magnetohydrodynamic (MHD) equations. The control problems associated with the diffusive evolution of the distributions of pressure and current density (a.k.a. profile control) can be reduced to a simpler diffusion partial differential equation. Distributed controllers for this system have been derived and rigorously analysed from different control theoretical perspectives [1–4]. Some profile control methods have been implemented and experimentally tested. In addition, a family of nonlinear oscillations exists in the plasma in which the profile evolution is limited by a crash-like reset event which is typically the consequence of nonlinear, resistive MHD activity. The sawtooth oscillation

 © 2016 IOP Publishing Ltd Printed in the UK

[10] and the edge-localized-mode (ELM) oscillation are the most relevant examples. The sawtooth oscillation is a periodic relaxation oscillation of all the relevant plasma variables (e.g. temperature, density, and pressure) in the center of the plasma. When a criterion for instability is met, the magnetic field in the centre reconnects in a crash-like event, causing a variation in a number of the core plasma parameters. The rapid variation of the magnetic field potentially drives losses of energetic particles and can cause secondary instabilities (NTMs) that lead to magnetic islands that may even disrupt the plasma. As the sawtooth period τ_{per} on ITER is predicted to be several orders of magnitude larger than on the current tokamaks (around 50 s), reliable control of this sawtooth period τ_{per} is considered critical for successful operation of ITER. The control of NTMs has been successful, both theoretically [5, 6] and experimentally [7, 8] and also [9] and references therein. The ELM oscillation is an oscillation that occurs at the edge of the plasma. As with the sawtooth, the ELM cycle is characterized by a slow evolution of the plasmas conditions until an instability criterion is met, after which a crash-like reset of the plasma conditions occurs. Subject to the experimental conditions, the ELM crashes are periodic or chaotic. The crashes are associated with high dynamic heat fluxes to the reactor wall. Notably long ELM crash periods are expected to cause severe damage, and ELM period control [11, 12] is considered important for ITER operations. Systematic ELM feedback control on JET is presented in [13]. Also systematic sawtooth period controller design was done, but to our knowledge, no purely theoretic analyses have been carried out on ST period control or for ELMs. However, for sawtooth period control, several control approaches have been studied by a combination of theory and simulations: PID control [14] and extremum seeking control [15]. Earlier, also other experiments, with feedback control of the sawtooth period, have been performed [16–20]. All these experiments controlled the sawtooth period by controlling the precise location where power was deposited by means of electron/ion cyclotron resonance heating/current drive.

Recently, another perspective on sawtooth period control has emerged. Instead of changing the power deposition location, the location is fixed and the power itself is modulated in time. This approach has been successfully tested in experiments on TCV [21, 22] and FTU [23] and has also been simulated for TEXTOR and TCV conditions [25]. Recent simulations [24] show that power modulation can also be feasible for sawtooth control on ITER. The power modulation approach can be divided in two types: (1) in [22, 24, 25] the period of the power modulation is chosen reasonably close to the natural sawtooth period. This results in period locking of sawtooth period, i.e. the sawtooth period τ_{per} adapts to the modulation period. The mode locking phenomenon is very common in nonlinear oscillations and can be used as an open-loop controller. Although open-loop control is not adaptable to changing circumstances, the possibility to operate in the absence of real-time measurements can be advantageous, especially in future DEMO tokamaks where making real-time measurements will be extremely difficult. (2) Contrary to the former type, the second method, pacing control, uses a feedback loop. Immediately after each sawtooth crash the power is decreased to zero for a finite time τ_{set}, where $\tau_{\text{set}} \leqslant \tau_{\text{per}}$. For $t > \tau_{\text{set}}$, with time t set to zero at the moment of the sawtooth crash, the power is instantaneously increased to a constant value, for the time remaining until the next sawtooth crash. The power modulation is adapted according to the following linear feedback law [26]

$$\tau_{\text{set}}, k = \tau_{\text{set}}, k-1 + K(\tau_{\text{ref}} - \tau_{\text{per}}, k-1), \tag{1}$$

where τ_{ref} is a (constant) desired reference period and $K \in \mathbb{R}$ a control parameter. The discrete time $k \in \mathbb{N}$ counts the number of sawtooth (or ELM) crashes, which corresponds to crash or reset times t_k, $k \in \mathbb{N}$. Note that in [26] there is also a feedforward term in the pacing control law to achieve faster convergence to τ_{ref}. Here, the feedforward term is neglected. In [27] experimental results of pacing and locking control of both ELM and sawtooth periods on JET are presented.

The contribution of this paper is twofold. First we show that the sawtooth period dynamics can be modeled by a simple reduced model. This model is a first order reset equation, which resembles an *integrate-and-fire* model (which is used as the simplest dynamical model of a neuron). Perhaps not coincidentally, a model with mathematically similar characteristics has been proposed for ELM oscillations at TCV [26]. Then the period dynamics is explicitly modeled as a nonlinear discrete-time map. When the pacing controller (a discrete-time control law) is applied to this map, a Lur'e system [30] appears. This implies that the system can be decomposed into a linear system with a static nonlinearity in negative feedback. The nonlinearity can be bounded by a sector and this leads to conditions for which the controlled system is globally exponentially stable. Because of the robustness in this approach, the results hold even if the reduced model is just a coarse approximation of the real dynamics.

The structure of the remaining paper is as follows. In section 2, the sawtooth model is introduced. In section 3 that model is reduced to a reset model and in section 4 we will analyse pacing control. Finally, conclusions are drawn.

2. The sawtooth model

The magnetic field $\vec{B}(x, y, z, t)$ in a tokamak is decomposed into the toroidal B_ϕ and poloidal B_θ field and R are the major radius and r_{pol} the radius of the poloidal plane. Under the assumption that the field is axisymmetric, the field is characterized by the q-profile which can be approximated by

$$q(r, t) = \frac{rB_\phi}{RB_\theta}, \tag{2}$$

if the tokamak is circular and has a large-aspect-ratio. Here B_ϕ is assumed to be constant for simplicity. The q-profile $q(r, t)$ at radius r can be interpreted as the inverse winding number of the field lines that lie on the flux surface with radius r, as can be seen in figure 1. Many instabilities in the magnetic field,

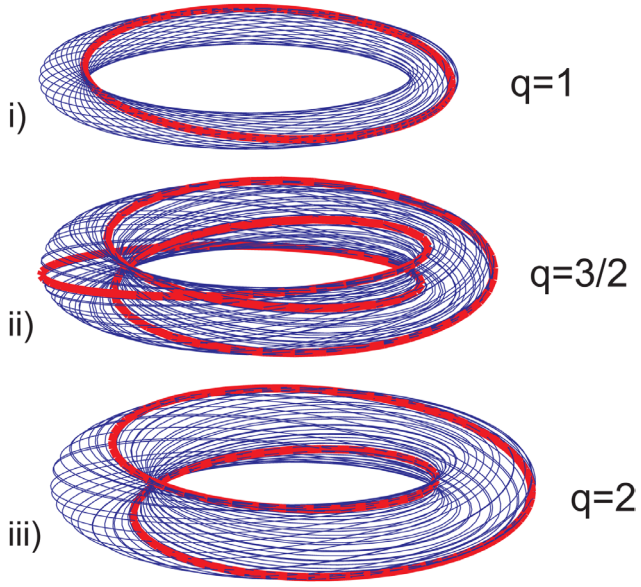

Figure 1. Three examples of flux surfaces. The q number indicates that, for any magnetic field line on the flux surface, the field line rotates around once in poloidal direction for every q toroidal rotations. The sawtooth oscillation is related to the behavior in the neighborhood of the $q = 1$ flux surface.

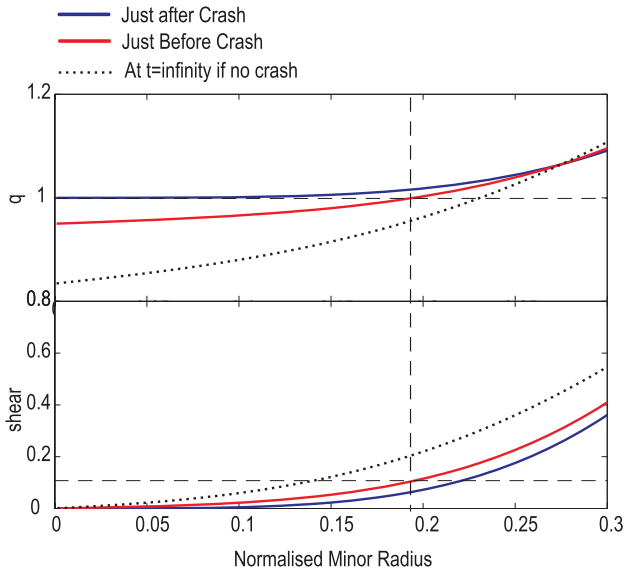

Figure 2. The evolution of the q-profile. Just before the crash, $r(q = 1) = 0.19$ and the shear at that location is equal to the critical shear c_3. Observe that the q-profile just before the crash is still far from the stationary state (at $t \to \infty$), which is never reached because of the sawtooth crash.

and associated reconnection, occur at places where q is a strong rational number $m : n$, with $m, n \in \mathbb{N}$. For example, the NTMs typically occur at places where $q = 2 : 1$ or $3 : 2$, while the sawtooth crash originates at the $q = 1 : 1 = 1$ surface.

In the time between two sawtooth crashes, the q-profile evolves diffusively. According to the model of Porcelli [14, 31], the exact moment that the sawtooth crash occurs depends on the shear

$$s(r,t) = \frac{r_{\text{pol}}\mathrm{d}q}{q\mathrm{d}r} = 1 - \frac{r\mathrm{d}B_\theta}{B_\theta \mathrm{d}r} \tag{3}$$

at the flux surface where $q = 1$. Therefore,

$$s_1(r(q=1),t) = \frac{r\mathrm{d}q}{\mathrm{d}r}. \tag{4}$$

As $q(r, t)$ evolves according to a diffusion equation of B_θ [14], also the shear $s_1(r(q = 1), t)$ evolve diffusively. It is important to note that the q-profile, and hence $s(r, t)$, does not evolve diffusively towards a spatially constant $q(r, t)$ profile, as would be expected for a diffusion equation, but towards a stationary profile like in figure 2. This is due to the fact that it is the electric field that diffuses and this determines, by a complex relation, the q-profile. Moreover, the q-profile never reaches this stationary profile, because at the moment that the shear is equal to the critical shear, $s_1(t) = c_3$, the magnetic field inside $r(q = 1)$ reconnects and most plasma variables suddenly drop, as can be seen in figure 3. The critical shear c_3 actually is a function of time, but in many cases it can be assumed constant. This assumption is also applied here. In figure 2 the q-profile is shown just before the crash (red) and just after the crash (blue). The stationary solution (dotted) of the diffusive process is clearly much lower than these but is never reached, as the q-profile resets long before this solution is achieved.

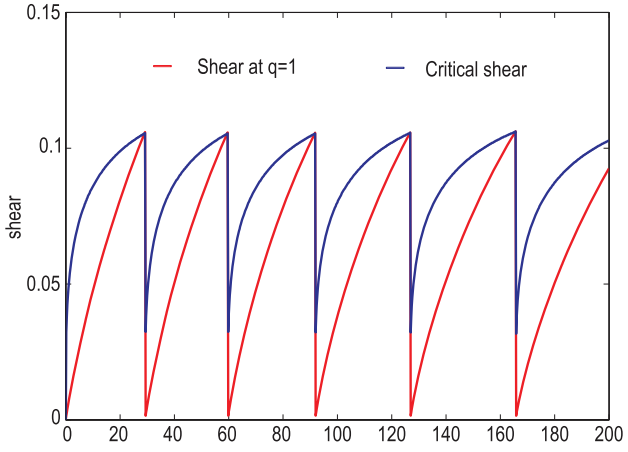

Figure 3. Simulations of the shear evolution at $r(q = 1)$ and the critical shear c_3 as a function of time. Observe that the maximal and minimal value are approximately the same for every period. In this work, c_3 and c_2 are therefore assumed constant. To reproduce the shown sawtooth period the values have to be $c_3 = 0.105$ and $c_2 = 0.001$.

3. A control-oriented model

In the former section the physics behind the sawtooth oscillation has been shown. Note that although the physics based model of the sawtooth oscillation, as given in [14], is a complex partial differential equation, in figure 3 the shear at $q = 1$ appears to repeatedly evolve exponentially. Here, we will motivate a model based on a simplification of the exposed physics.

Observe that figures 2 and 3 show that the shear s_1 at $q = 1$ increases towards a stationary but nonzero value. This evolution is modeled by a diffusion equation [14] with time and space dependent parameters and a reset, and in one cylindrical

coordinate. As an approximation, we assume that on the relevant length scale the parameters such as the resistivity are constant and we approximate the cylindrical coordinate r by a Cartesian coordinate z. We postulate that diffusion will eventually lead to a steady state shear profile $s(z)_{ss} = b$, on a length scale l smaller than the minor radius r_{per}. This locally approximates the critical shear value c_3. Now, a simplified 1D diffusion equation can be introduced that mimics the diffusive shear evolution (caused by the diffusion of the q-profile)

$$\frac{\partial s}{\partial t} = \frac{\eta}{\mu_0}\frac{\partial^2 s}{\partial z^2}, \tag{5}$$

on the spatial domain $[0, l]$, with a constant resistivity η [14], the vacuum permeability $\mu_0 = 4\pi \cdot 10^{-7}$, and Dirichlet boundary conditions $s(0, t) = s(l, t) = c_0/c_1$, where the constants c_0 and c_1 depend on the initial profile. So it is assumed that the shear at $q = 1$ evolves towards a nonzero value in steady-state. Therefore, the diffusion of $s(z, t)$ is relevant for computing the time (i.e. the sawtooth period τ_{per}) it takes the shear at $q = 1$ to reach the critical shear $c_3 < c_0/c_1$. Now, $s(z, t)$ can be approximated by using Fourier modes

$$s(z, t) = \sum_{i=1}^{N} \alpha_i(t) \sin\left(\frac{i\pi z}{l}\right), \tag{6}$$

where $N \in \mathbb{N}$ is the truncation order. Moreover, note that for any given Fourier mode $s(z, t)_i = \alpha_i(t) \sin(\frac{i\pi z}{l})$ it holds that

$$\frac{\partial^2 s(z, t)_i}{\partial z^2} = -\alpha_i(t)\frac{i^2\pi^2}{l^2} \sin\left(\frac{i\pi z}{l}\right). \tag{7}$$

Assuming we are only interested in the first Fourier mode $i = 1$, as this is the slowest mode with the longest length scale, we can derive that the amplitude of this mode evolves as a first-order system

$$\alpha_1(t) = \alpha_1(0) \exp\left(-\frac{\eta\pi^2}{l^2\mu_0}t\right). \tag{8}$$

This is physically sensible, as it implies evolution on the diffusive time scale $l^2\mu_0/\pi^2\eta$, for the length scale l.

Assuming nonzero steady-state shear and truncating the associated diffusion equation to the slowest mode, the previous model reduction motivates that evolution of the shear at $q = 1$ is evolving as a first order system towards a nonzero value c_0/c_1. This can be written as

$$\dot{x} = c_0 - c_1 x + v, \tag{9}$$

where state x is the shear at $q = 1$ and where v is the contribution to the shear at $q = 1$ from the first spatial mode of the input (by ECCD), $c_1 = \eta\pi^2/l^2$, and c_0/c_1 is related to the steady state of the shear. Figure 4 shows the simulated effect of stabilizing ECCD on the shear at $q = 1$ and on the critical shear. In equation (9) the critical shear variation is neglected while the effect of ECCD on the shear at $q = 1$ is represented by v.

Using these observations, the sawtooth crash can now be modeled as a reset condition. Once the shear-related state x equals the critical shear c_3, the profile and thereby x is reset to a smaller value c_2. Observe that under the circumstances of the simulation in figure 3, the values are $c_2 = 0.001$ and $c_3 = 0.105$. Hence, assembly of these model components leads to the reset model

$$\begin{aligned} \dot{x} &= c_0 - c_1 x + v \\ x^+ &= c_2 \text{ when } x = c_3, \end{aligned} \tag{10}$$

with positive constants $c_1, c_2, c_3, c_4 > 0$ and an input variable v. The meaning of this model is that the state x evolves according to the differential equation until the condition $x = c_3$ is satisfied, at which moment the state is instantaneously reset to c_2, therefore the name reset model. We observe that a different, but mathematically comparable, ad hoc ELM period model has been suggested by Felici *et al* [26].

As a side note and before continuing with the model and the pacing analysis: it has been observed in several experiments and simulations [22–25] that the sawtooth period adapts to the period of modulated ECCD or ICRH, if the modulation period is close enough to the natural sawtooth period. This is a nonlinear phenomenon, called period locking, and the literature of leaky-integrate-and-fire neurons in neuroscience [28] analytically shows under which circumstances period locking occurs for this family of models. For sawteeth oscillations it is interesting to see that in the same literature it is shown that locking can also occur when the the reset value c_3 is time-varying or influenced by an input [29]. This is what is probably observed in experiments where the sawtooth period locks to modulated ICRH, as the fast particles created by ICRH are known to change c_3. This is relevant for ITER, as it is possible that due to fast particle effects ECCD alone will be insufficient to shorten the sawtooth period. In that case, ICRH can be used as a second input for pacing or locking control, as it either influences the fast particle population (and thereby c_3) or directly influences the shear at $q = 1$.

The model (10), with $v = 0$, predicts an exponentially converging evolution of the shear towards a constant nonzero value c_0/c_1. The shear is reset before this steady-state value is reached, because $c_2 < c_3 < c_0/c_1$, leading to a periodic fast-slow oscillation. Observe that this is consistent with the evolution shown in the simulation in figure 3.

Remark 3.1. The occurence of fast particles can influence the MHD stability of the internal kink mode and thereby influence the sawtooth crash [31]. This contribution of fast particles could also be modeled by making the reset condition c_3 time-dependent, and in experiments [32, 33] $c_3(t)$ can be influenced by using another input, e.g. ion cyclotron resonance heating (ICRH). Here, this effect will not be taken into account, but a similar analysis can in principle be carried out.

The reduced reset model in (10) is suited for (pacing) control analysis. The pacing control setup, as discussed in the introduction, see (1), simplifies the admissible profile for the input v, as it assumes only two possible values for the input

$$v(\tau) = \begin{cases} 0, & \text{if } 0 \leqslant \tau \leqslant \tau_{set} \\ v_{max}, & \text{if } \tau_{set} < \tau, \end{cases} \tag{11}$$

with v_{max} being proportional to the applied gyrotron power of the ECCD. Observe that the sign of v_{max} depends on whether the ECCD is stabilizing or destabilizing, resulting in respectively a negative and a positive sign. Furthermore, τ is a timer

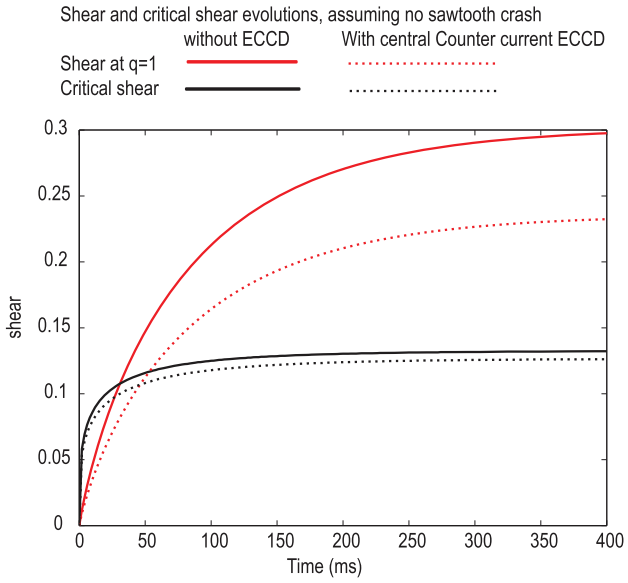

Figure 4. Evolution of the shear at $r(q = 1)$ and the critical shear, with (dotted line) and without (line) counter current ECCD. The current leads to the shear decrease during the evolution, implying that $v(t)$ has a negative sign for these simulations.

that starts at zero at the beginning of every sawtooth period. Hence, the only variable in the choice of the input signal v is τ_{set}. For the control analysis, the notation is changed to be conform with the control literature; the input is now denoted $u = \tau_{\text{set}}$ (which is the time during which the power is decreased to zero after the crash) and the output (i.e. the sawtooth period τ_{per}) is denoted as $y = \tau_{\text{per}}$. In fact, we are going to consider u and y on discrete times, labeled by $k \in \mathbb{N}$, and corresponding to the crash/reset times t_k, $k \in \mathbb{N}$. Hence, we are going to write u_k and y_k as the kth control input and the kth ouput (sawtooth period). The reference period in (1) becomes $r = \tau_{\text{ref}}$, which is the required period.

Remark 3.2. Assuming pacing control (1) and (11), the model (10) can be rewritten formally in the hybrid system framework advocated in [34]. The flow dynamics are given by

$$\dot{x} = \begin{cases} c_0 - c_1 x, & \text{if} \quad 0 \leqslant \tau \leqslant u, \\ c_0 + v_{\max} - c_1 x & \text{if} \quad u < \tau \leqslant \tau_{\text{per}}, \end{cases} \tag{12}$$

$$\dot{\tau} = 1, \quad \dot{u} = 0, \quad \dot{s} = 0, \tag{13}$$

when $0 < x \leqslant c_3$. The variable s is redefined here to store the previous sawtooth period and the timer τ is tracking the time elapsed since the last reset. The jump dynamics is given by

$$\begin{aligned} x^+ &= c_2, \\ \tau^+ &= 0, \\ u^+ &= u + K(r - s), \\ s^+ &= \tau, \end{aligned} \tag{14}$$

when $x = c_3$. Here, u is assumed to adapt according to (1), and we assume for ease of exposition that $v_{\max} > 0$. An interesting feature of the control problem for this hybrid systems is that we are interested in the control of the time between resets, which is not often considered in the hybrid literature, see, e.g. [34].

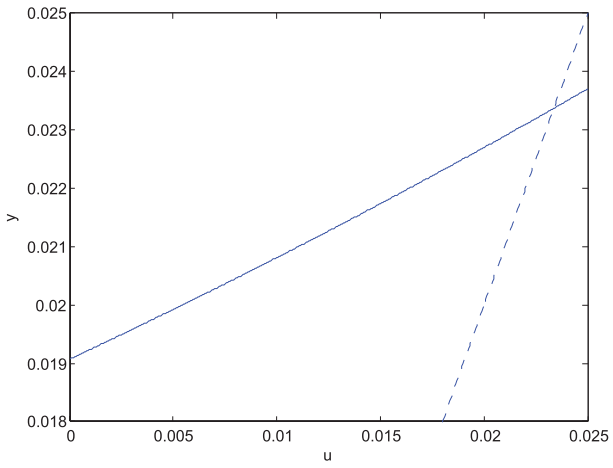

Figure 5. The almost linear input–output map from u_k to y_k (solid) and the diagonal $u = y$ (dotted). For the parameters $v_{\max} = 1, c_0 = 5, c_1 = 10, c_2 = 0.001, c_3 = 0.105$ the autonomous sawtooth period (with $u = 0$) is approximately $\tau_{\text{per}} = 19$ ms.

To solve the problem of controlling the duration between two resets, we are going to compute the influence of the pacing time u_k on the sawtooth period y_k in two steps. In particular, we are going to consecutively solve the two equations in (12) over the time interval $[0, u_k]$ and $(u_k, y_k]$, respectively. Solving (12) for $\tau \in [0, u_k]$ (and thus $t \in [t_k, t_k + u_k]$) leads to

$$x(\tau) = (c_2 - c_0/c_1)\mathrm{e}^{-c_1\tau} + c_0/c_1. \tag{15}$$

At $\tau = u_k$ the state x is

$$x(u_k) = (c_2 - c_0/c_1)\mathrm{e}^{-c_1 u_k} + c_0/c_1. \tag{16}$$

For $\tau \in [u_k, y_k]$ (and thus $t \in [t_k + u_k, t_{k+1}]$) the solution of (12) is

$$x(\tau) = \mathrm{e}^{-c_1(\tau - u_k)}\left(x(u_k) - \frac{c_0 + v_{\max}}{c_1}\right) \tag{17}$$

$$+\frac{c_0 + v_{\max}}{c_1}. \tag{18}$$

Because $x(y_k) = c_3$ (note that $t_k + y_k = t_{k+1}$) by definition of the reset, it follows that

$$c_3 = \mathrm{e}^{-c_1(y_k - u_k)}((c_2 - c_4)\mathrm{e}^{-c_1 u_k} + c_6) + c_5 \tag{19}$$

with $c_4 := c_0/c_1$, $c_5 := (c_0 + v_{\max})/c_1$ and $c_6 := c_4 - c_5$. Therefore, the sawtooth period y_k can be expressed explicitly as a stationary nonlinear map, see figure 5, of u_k, i.e.

$$\begin{aligned} &y_k = \tilde{g}(u_k), \text{ with} \\ &\tilde{g}(u_k) = u_k - \frac{1}{c_1}\ln\left(\frac{c_3 - c_5}{(c_2 - c_4)\mathrm{e}^{-c_1 u_k} + c_4 - c_5}\right). \end{aligned} \tag{20}$$

Note that the above derivation only makes sense when $u_k \geqslant 0$. In fact, we denote $\tilde{g}(0)$ as $y_{\min}$ as this is the smallest value of the period that can be realized (corresponding to maximal power $v(t) = v_{\max}$ for all the time). Moreover, if we use $v(t) = 0$ all the time, then the system will experience a reset period denoted by $y_{\max}$, the maximal period that can be realized. Hence, values of u_k outside the domain $[0, y_{\max}]$ are meaningless and the corresponding reset periods y_k can only

be realized for values of $u_k \in [0, y_{\max}]$, $k \in \mathbb{N}$. Therefore, we use saturation of u_k when it is outside the domain $[0, y_{\max}]$ and we modify the function $\tilde{g}$ to g given for $u_k \in \mathbb{R}$ by

$$g(u) = \begin{cases} y_{\min}, & \text{if} \quad u < 0 \\ \tilde{g}(u), & \text{if} \quad 0 \leqslant u \leqslant y_{\max} \\ y_{\max}, & \text{if} \quad u > y_{\max}. \end{cases} \tag{21}$$

Hence, we obtain

$$y_k = g(u_k). \tag{22}$$

4. Pacing control analysis

Pacing control can now be analysed by substituting the pacing control law

$$u_{k+1} = u_k + K(r - y_k), \tag{23}$$

which results in the nonlinear discrete-time dynamics

$$u_{k+1} = u_k + K(r - g(u_k)). \tag{24}$$

Remark 4.1. A few remarks are in order here. First, the measured sawtooth period y_k is needed in the pacing control law (23). In experiments, because of the high amount of measurement noise, the computation of the sawtooth period is not trivial and takes significant time [35]. Typically, one or two sawtooth periods are needed for TCV or TEXTOR circumstances, while the detection delay is negligible on bigger machines such as JET and Tore Supra. This time-delay effect is neglected here, but can be taken into account by using y_{k-n}, with a small $n \in \mathbb{N}$, in the pacing control law (1) instead of y_k. Second, the period dynamics in (24) is based on the simplified model (10), but the following approach remains valid when the period dynamics would be given by a different map g, as long as it satisfies certain properties. In fact, this robustness, that we will show below analytically in theorem 4.1, makes the pacing control a successful strategy.

For the function g, for which an example was depicted in figure 5 we adopt the following assumption.

Assumption 4.1. The map $g : \mathbb{R} \to \mathbb{R}$ is monotonically increasing and in the region $(y_{\min}, y_{\max})$ it is strictly increasing. Moreover, g is continuously differentiable on $(y_{\min}, y_{\max})$ and there are constants $d_{\max} > d_{\min} > 0$ such that for all $u \in (y_{\min}, y_{\max})$ it holds that $d_{\max} > g(u) > d_{\min}$.

We are now studying the periods that can be realized and in fact as set-points we restrict ourselves to the reference periods within the physically reasonable interval

$$r \in \Omega_r := (y_{\min} + \delta, y_{\max} - \delta), \tag{25}$$

with a small $\delta > 0$ and $0 < y_{\min} < y_{\max}$. Clearly under the assumption 4.1 the dynamics (24) have a unique equilibrium u_r^* (depending on r) for each $r \in \Omega_r$ satisfying $g(u_r^*) = r$.

To study the stability of the equilibrium u_r^*, we will study the error dynamics for the error defined as $e_k := u_k - u_r^*$, for $k \in \mathbb{N}$. This error dynamics is given by

$$e_{k+1} = e_k - K(g(u_r^* + e_k) - r). \tag{26}$$

As $g(u_r^*) - r = 0$, $e_k = 0$ is the equilibrium of (26). To study the stability, we assume that the initial value for the input is within the physically reasonable domain $[0, y_{\max}]$, i.e.

$$u_0 \in [0, y_{\max}] \tag{27}$$

and therefore

$$|e_0| = |u_0 - u_r^*| \leqslant y_{\max}. \tag{28}$$

The domains on which e and u are considered are denoted by

$$\Omega_e = \{e \in \mathbb{R} \mid |e| \leqslant y_{\max}\}, \tag{29}$$

$$\Omega_u = \{u \in \mathbb{R} | u \in (-y_{\max}, 2y_{\max})\}. \tag{30}$$

The system (26) can now actually be conceived as a Lurie system [30, 36], i.e. the interconnection of a linear system in feedback with a nonlinearity (for each fixed r). To be more precise, a discrete-time Lurie system can be written as the linear system

$$x_{k+1} = Ax_k + Bw_k, \tag{31}$$

$$\theta_k = Cx_k. \tag{32}$$

In which $x_k \in \mathbb{R}^n$ denotes the state, $w_k \in \mathbb{R}^m$ the input and $\theta_k \in \mathbb{R}^p$ the output at discrete time $k \in N$, interconnected with the nonlinear mapping

$$w_k = -\phi(\theta_k). \tag{33}$$

A, B and C are constant matrices of appropriate dimensions and $\phi : \mathbb{R}^p \to \mathbb{R}^m$. In our case $p = m = n = 1$ and ϕ will depend on the fixed value of r.

Hence, we can write (32) and (33) compactly as

$$x_{k+1} = Ax_k - B\phi(\theta). \tag{34}$$

Due to the assumption 4.1 and use of the mean value theorem, we can show that there exist bounds $\underline{\gamma}$ and $\overline{\gamma}$ with $0 < \underline{\gamma} < \overline{\gamma}$ such that for all $e \in \Omega_e$ and $r \in \Omega_r$

$$\underline{\gamma} e \leqslant g(u_r^* + e) - r \leqslant \overline{\gamma} e. \tag{35}$$

This implies that the nonlinearity is sector bounded, i.e. the map is lower- and upper-bounded by a linear function. Numerical values for $\underline{\gamma}$ and $\overline{\gamma}$ can be found by simulating or experimentally measuring the input-output map $y_k = g(u_k)$ of real sawtoothing or ELMing plasmas for a number of feasible values of u and then finding linear lower- and upperbounds for the map.

In fact, the bounds $\underline{\gamma}$, $\overline{\gamma}$ can be related to $d_{\min}$ and $d_{\max}$ in assumption 4.1. Hence, we have a Lur'e system with a sector bounded nonlinearity in the feedback path and the sector is given by $[\underline{\gamma}, \overline{\gamma}]$. As a consequence, we can rewrite the error dynamics (26) as the the error evolution

$$e_{k+1} = (1 - K\gamma_k)e_k \tag{36}$$

with $\gamma_k \in [\underline{\gamma}, \overline{\gamma}]$ for each $k \in \mathbb{N}$. Clearly, this system can be analysed by considering the Lyapunov function $V(e) = |e|$ and from this we obtain that if $|1 - K\gamma_k| < 1$ for all $k \in \mathbb{N}$, then we have global exponential stability (GES) of the equilibrium $e = 0$ (correpsonding to $u = u_r^*$ and $y = r$) and positive invariance of Ω_e and Ω_r for the respective variables, i.e. $e_k \in \Omega_e$ and

$u_k \in \Omega_u$ for all $k \in \mathbb{N}$. Hence, this puts a condition on the gain K given by

$$0 < K < \frac{2}{\overline{\gamma}}. \tag{37}$$

If $g(u)$ satisfies (22) we have established the following result.

Theorem 4.1. *Consider the dynamics given by (24) and assume that the function g satisfies assumption 4.1 and $r \in \Omega_r$. Then there exist $0 < \underline{\gamma} < \overline{\gamma}$ such that (35) holds for all $e \in \Omega_e$ and all $r \in \Omega_r$. If, in addition, K satisfies (37), then for any fixed value of $r \in \Omega_r$ the corresponding u_r^* is a GES equilibrium for the dynamics (24) for any $u_0 \in [0, y_{\max}]$.*

Three remarks are in order. First of all recall that if u_k converges to u_r^*, that then y_k converges to r, as desired. Second, interestingly, the result in theorem 4.1 is independent of the actual value or r. So, if another value of $r \in \Omega_r$ and u_r^* is taken the system (24) will converge to this value as well and even slowly-varying time-dependent trajectories of r can be tracked. Third, even if g differs from the one that we computed in (20), but g still satisfies the conditions of the theorem, then the same conclusions regarding stability can be drawn. Hence, the theorem holds for any g satisfying assumption 4.1 indicating the robustness of the pacing control strategy.

Remark 4.2. If $0 < K < 1/\overline{\gamma}$, then it holds that e_k does not change sign over time and smaller positive invariant sets for e and u can be derived.

Basically, this means that if the variable of interest is inside the set at some point of time, the variable of interest will remain inside the set for all future values of time

Remark 4.3. Note that we can even provide guarantees on the speed that $|u_k - u_r^*|$ converges to zero when k goes to ∞. The convergence factor is given by $\max(|1 - K\overline{\gamma}|, |1 - K\underline{\gamma}|)$.

These theoretical results have straightforward implications for the tuning of pacing controllers in real experiments. Assuming that the input-output map (22) is known from experiments or simulations or analysis, one can tune the pacing gain K such that pacing control is guaranteed to be stable. Moreover, given certain values for the sector bounds $\underline{\gamma}$ and $\overline{\gamma}$ one can tune K such that the error quickly converges to zero. If the acquired input-output map is rather uncertain or tends to change over different experiments, it is important to chose the sector bounds more conservatively, resulting in slower convergence. As often in feedback control, a balance between performance and robustness must be found when the model is not entirely reliable. Note that these results does not depend on whether the reset model (10) is correctly describing the sawtooth or ELM period dynamics or not. If it does, then that model can be used for deriving the input-output map analytically but also for designing open-loop inputs that result in period locking.

5. Conclusions

The efficiency and safety of fusion plasmas in tokamaks often deteriorates by the occurrence of certain relaxation oscillations in the relevant fields. The period of the two most important oscillations, the sawtooth and the ELM oscillation, have been successfully controlled in experiments by application of the so-called pacing control law. This controller depends only on one control parameter K. For the sawtooth oscillation a complex theoretical model exists, which consists of a linear parameter-varying partial differential equation and a state-dependent reset.

In this contribution we first motivated that the dynamics of this model can be reduced to a first order differential equation with reset. This model predicts sawtooth period locking, which has previously been observed in experiments and simulations. Secondly, the dynamics of the sawtooth period with pacing control is written as a nonlinear discrete-time system. This system can be perceived as a Lur'e system, i.e. a linear system with a static nonlinearity in the negative feedback path. By deriving the sector bounds to the nonlinearity (which is always possible for the nonlinearities at hand), as we showed we can prove that the complete system is globally asymptotically stable for a finite range of K. To the best knowledge of the authors, this is the first completely theoretical analysis resulting in conditions that guarantee that the control law will indeed guarantee global exponential stability of the desired reference sawtooth period.

This result not only implies that pacing control leads to a desired sawtooth period when the control parameter K is chosen appropriately. In addition, this result is independent of the chosen setpoint (desired period) and in fact, will also work for slowly varying setpoints. Moreover, the result is extremely robust for model perturbations and uncertainties. As long as the perturbed model satisfies the sector conditions and the monotonicity requirements, the methodology and results apply. This is essential, as the physical mechanisms that are responsible for the sawtooth oscillation are time-varying and can be more complex than the reduced model as used here.

Having developed this reset model for sawtooth pacing it would be interesting to investigate the possibility of developing a similar model for the pacing of another important MHD phenomenon: edge localised modes (ELMs). Even though we do not fully understand the nonlinear crash mechanism for the ELMs, it is clear that the evolution is often qualitatively similar to the sawtooth phenomenon. The equivalent of the current diffusion phase is a phase where the pressure, pressure gradient, electric fields etc at the edge evolve slowly. This evolution can (as most slow evolutions) be approximated well by a first order evolution. Higher order components will only play a small role in determining the time taken to arrive at the crash criteria, but from a feedback control perspective this precise information is often not necessary, as the feedback control law compensates for the measured difference between model and measurement.

As, the non-linear physics of the sawtooth crash is ignored in the sawtooth model, the non-linear physics during the ELM crash can also be ignored and the ELM can be considered to instantaneously return the plasma to the initial state. What is missing is a universal formulation of the ELM crash criteria (the Porcelli criterion is anyway not necessarily correct, especially in the presence of fast ions). It is however clear that such a criteria exists and like the sawtooth criteria it can depend on a number of plasma parameters, though the dependences

are not well known at the moment. From these considerations it is reasonable to expect that a reset model, very similar to the one described in this paper, could be applied directly to the ELM phenomena by changing a few parameters such as the time constant of the inter ELM evolution and the level of the critical parameter at which an ELM crash occur. In [26], a mathematically comparable model has already been suggested to model the reaction of ELM periods to ECCD power modulation in TCV plasmas.

Experiments have shown that ELM pacing can be done by introducing sharp perturbations. These perturbations are equivalent of the sharp increase in the shear at $q = 1$ induced by ECCD in the Sawtooth model. Further work would be required to put such an ELM model on a solid foundation, but based on the above analysis it is likely that such a model will lead to similar results regarding pacing range and convergence as seen for the sawtooth pacing model. We envision that the results for pacing control of the sawtooth period also apply for pacing control of the ELM period in the specific regime. However, we explicitly note that the theoretical analysis of pacing control in section 4 does not depend on the validity of the reset model for ELMs.

Moreover, both our sawtooth model and the ELM model [26] resemble the *integrate-and-fire* model, used in neuroscience as the most simple model for neurons. This suggests that our analysis of pacing control might also be applicable to period control of neurons. Several theoretical methods have been suggested in that field, but the simplicity and robustness of pacing might be beneficial for application in experiments.

For future work, the analysis of pacing control with a time-dependent reset condition $c_3(t)$, instead of constant c_3, is relevant for experiments. This is especially true when a second actuator (ICRH) is used that influences the evolution of $c_3(t)$, which can be relevant for ITER in case ECCD is insufficient to shorten the sawtooth period. Furthermore, the analysis here depends on a reset model that incorporates only one Fourier mode of the original diffusion equation. Therefore, a more detailed analysis including a larger but finite number of Fourier modes in the reset model would certainly be of interest. As this model will still have a Lur'e form, the same type of stability analysis as reported here could be performed to study whether the addition of these (faster) modes is needed or not. For experiments it would be relevant to study the influence of significant time delays, caused by the measurement of the sawtooth period, on the stability and performance of pacing control.

Acknowledgments

The authors thank C Criens and E Witrant for helpful discussions. This work has been carried out within the framework of the EUROfusion Consortium and has received funding from the Euratom research and training programme 2014–2018 under grant agreement No 633053. The views and opinions expressed herein do not necessarily reflect those of the European Commission.

References

[1] Argomedo F B, Witrant E, Prieur C, Brémond S, Nouailletas R and Artaud J-F 2013 Lyapunov-based distributed control of the safety-factor profile in a tokamak plasma *Nucl. Fusion* **53** 033005

[2] Boyer M D, Barton J, Schuster E, Luce T C, Ferron J R, Walker M L, Humphreys D A, Penaflor B G and Johnson R D 2013 First-principles-driven model-based current profile control for the DIII-D tokamak via LQI optimal control *Plasma Phys. Control. Fusion* **55** 105007

[3] Felici F and Sauter O 2012 Non-linear model-based optimization of actuator trajectories for tokamak plasma profile control *Plasma Phys. Control. Fusion* **54** 025002

[4] Maljaars E, Felici F, de Baar M R, van Dongen J, Hogeweij G M D, Geelen P J M and Steinbuch M 2015 Control of the tokamak safety factor profile with time-varying constraints using MPC *Nucl. Fusion* **55** 023001

[5] Hennen B A, Lauret M, Hommen G, Heemels W P M H, de Baar M R and Westerhof E 2012 Nonlinear control for stabilization of small neoclassical tearing modes in ITER *Nucl. Fusion* **52** 063007

[6] Wehner W and Schuster E 2012 Control-oriented modelling for neoclassical tearing mode stabilization via minimum-seeking techniques *Nucl. Fusion* **52** 074003

[7] Hennen B A, Westerhof E, Nuij P W J M, Oosterbeek J W, de Baar M R, Bongers W A, Bürger A, Thoen D J and Steinbuch M 2010 Real-time control of tearing modes using a line-of-sight electron cyclotron emission diagnostic *Plasma Phys. Control. Fusion* **52** 104006

[8] Felici F, Goodman T P, Sauter O, Canal G, Coda S, Duval B P, Rossel J X and the TCV Team 2012 Integrated real-time control of MHD instabilities using multi-beam ECRH/ECCD systems on TCV *Nucl. Fusion* **52** 074001

[9] Marashek M 2012 Control of neoclassical tearing modes *Nucl. Fusion* **52** 074007

[10] von Goeler S, Stodiek W and Sauthoff N 1974 Studies of internal disruptions and $m = 1$ oscillations in tokamak discharges with soft x-ray tecniques *Phys. Rev. Lett.* **33** 1201

[11] Lang P T *et al* and JET-EFDA Contributors 2013 ELM pacing and trigger investigations at JET with the new ITER-like wall *Nucl. Fusion* **53** 073010

[12] Horton L D *et al* and the ASDEX Upgrade Team 2004 ITER-relevant H-mode physics at ASDEX Upgrade *Plasma Phys. Control. Fusion* **46** B511

[13] Lennholm M *et al* and JET EFDA contributors 2015 ELM frequency feedback control on JET *Nucl. Fusion* **55** 063004

[14] Witvoet G, Steinbuch M, de Baar M R, Doelman N J and Westerhof E 2012 Sawtooth period control strategies and designs for improved performance *Nucl. Fusion* **52** 074005

[15] Bolder J J, Witvoet G, de Baar M R, Van De Wouw N, Haring M A M, Westerhof E, Doelman N J and Steinbuch M 2012 Robust adaptive control of the sawtooth instability in nuclear fusion *Proc. American Control Conf.* pp 5023–8

[16] Lennholm M *et al* 2009 Closed loop sawtooth period control using variable ECCD injection angles on tore supra *Fusion Sci. Technol.* **55** 45–55

[17] Graves J P, Chapman I T, Coda S, Johnson T, Lennholm M, Paley J I and Sauter O 2011 Recent advances in sawtooth control *Fusion Sci. Technol.* **59** 539–48

[18] Chapman I T 2011 Controlling sawtooth oscillations in tokamak plasmas *Plasma Phys. Control. Fusion* **53** 013001

[19] Paley J I, Felici F, Coda S, Goodman T P, Piras F and the TCV Team 2009 Real time control of the sawtooth period using EC launchers *Plasma Phys. Control. Fusion* **51** 055010

[20] Lennholm M *et al* and JET EFDA Contributors 2011 Feedback control of the sawtooth period through real time control of the ion cyclotron resonance frequency *Nucl. Fusion* **51** 073032
[21] Goodman T P, Felici F, Sauter O and Graves J P 2011 Sawtooth pacing by real-time auxiliary power control in a tokamak plasma *Phys. Rev. Lett.* **106** 245002
[22] Lauret M, Felici F, Witvoet G, Goodman T P, Vandersteen G, Sauter O, de Baar M R and the TCV team 2012 Demonstration of sawtooth period locking with power modulation in TCV plasmas *Nucl. Fusion* **52** 062002
[23] Nowak S *et al* and FTU Team 2014 Control of sawtooth periods by pulsed ECH/ECCD in the FTU tokamak *Nucl. Fusion* **54** 033003
[24] Kim D, Goodman T P and Sauter O 2014 Feedback control of the sawtooth period through real time control of the ion cyclotron resonance frequency *Phys. Plasmas* **21** 061503
[25] Witvoet G, Lauret M, de Baar M R, Westerhof E and Steinbuch M 2011 Numerical demonstration of injection locking of the sawtooth period by means of modulated EC current drive *Nucl. Fusion* **51** 073024
[26] Felici F, Rossel J X, Duval B P, Coda S, Goodman T P, Martin Y, Moret J-M, Sauter O and the TCV Team 2013 Real-time control of the period of individual ELMs by EC power on TCV *Nucl. Fusion* **53** 113018
[27] Lennholm M *et al* and JET contributors 2016 Real-time control of ELM and sawtooth frequencies: similarities and differences *Nucl. Fusion* **56** 016008
[28] Coombes S, Thul R and Wedgwood K C A 2012 Nonsmooth dynamics in spiking neuron models *Physica* D **241** 2042
[29] Chacron M J, Pakdaman K and Longtin A 2003 Interspike interval correlations, memory, adaptation, and refractoriness in a leaky integrate-and-fire model with threshold fatigue *Neural Comput.* **15** 253
[30] Lur'e A I 1957 Some Nonlinear Problems in the Theory of Automatic Control (London: H.M. Stationery Off)
[31] Porcelli F, Boucher D and Rosenbluth M N 1996 Model for the sawtooth period and amplitude *Plasma Phys. Control. Fusion* **38** 2163
[32] Lennholm M *et al* 2009 Demonstration of effective control of fast-ion-stabilized sawteeth by electron-cyclotron current drive *Phys. Rev. Lett.* **102** 115004
[33] Graves J P, Chapman I, Coda S, Eriksson L-G and Johnson T 2009 Sawtooth-control mechanism using toroidally propagating ion-cyclotron-resonance waves in tokamaks *Phys. Rev. Lett.* **102** 065005
[34] Goebel R, Sanfelice R G and Teel A R 2012 *Hybrid Dynamical Systems* (Princeton, NJ: Princeton University Press)
[35] van Berkel M, Witvoet G, de Baar M R, Nuij P W J M, Ter Morsche H G and Steinbuch M 2001 Real-time wavelet detection of crashes in limit cycles of non-stationary fusion plasmas *Fusion Eng. Des.* **86** 2908–19
[36] Liberzon M R 2006 Essays on the absolute stability theory *Autom. Remote Control* **67** 1610–44